Accepted Manuscript
Version of record at: https://doi.org/10.1002/celc.202200231

RESEARCH ARTICLE

Salt Solution Concentration Effects on the Electrochemical Impedance Spectroscopy of Poly(3,4-ethylenedioxythiophene) (PEDOT)

Peter Sitarik and David C. Martin* [a]

[a] P. Sitarik, Prof. D. C. Martin
Department of Materials Science and Engineering
The University of Delaware
Newark, DE, 19716 USA
E-mail: milty@udel.edu

Abstract: Poly(3,4-ethylenedioxythiophene) (PEDOT) has become a widely used modifier for biomedical electrodes because of its ability to significantly decrease the impedance at low frequencies (below 1 kHz). However, in past studies the role of the solution concentration (ionic conductivity) on the electrochemical impedance behavior has not been well established. Here we describe the electrochemical impedance spectroscopy of the conjugated polymer (PEDOT) using standard screen-printed electrodes and various standard salt (NaCl) solutions with known conductivities from 1.0E-2 S/cm to 3.1E-6 S/cm. Changing the conductivity of the salt solution used for impedance measurements had a dramatic influence on the experimentally obtained spectra. An equivalent circuit consisting of a constant phase element in series with a parallel resistor and second constant phase element was used to match and describe these systems. Our results make it possible to better elucidate the influence of electrode, solution, and polymer coating on the resulting impedance response.

Introduction

Electrochemical systems are highly sensitive to the conditions surrounding the individual electrodes as well as the overall medium being used. The conductivity of the electrolytic solution itself is simple to control and has large effects on the entire system. This is particularly important in the use of impedance spectroscopy where it has been found that changing solution conductivity through the use of unreactive salts causes drastic changes in the impedance spectra [1,2].

For bioelectronic device integration there is a need to decrease the impedance in the frequency range of 1 kHz and below where biological signals take place [3,4]. Therefore, it is particularly important to understand what affects the impedance in this region and how to best analyze data that is being generated and published.

Conductive polymer (CP) systems are commonly used to functionalize inorganic, metallic, and semiconducting devices that transport charge in the solid-state with electrons and holes. These polymers facilitate communication with organic, electrolytic systems that transfer charge ionically. Of those CPs in the literature 3,4-ethylenedioxythiophene (EDOT) polymerizes into the well-studied poly(3,4-ethylenedioxythiophene) (PEDOT) [5–7]. PEDOT has been used in biomedical devices, solar cells, organic transistors, and sensors [8–10]. The change in impedance is a common metric used to characterize the alteration of the electrode surface for both PEDOT and the many functional derivatives of PEDOT that have been synthesized to date [11,12]. In previous studies it has been recognized that the conductivity of the electrolyte has a dramatic impact on the impedance response measured for a specific system, however the detailed origins of this effect were not examined directly, making it difficult to obtain a fundamental understanding of the origin of the response. Here, we examined the impedance response of PEDOT films in solutions with a broad range of conductivities and were able associate specific components of the impedance behavior with particular elements of equivalent circuit models.

In this experiment standard NaCl solutions with conductivities ranging over four orders of magnitude from 3.125E-6 S/cm to 1.00E-2 S/cm were tested with a selection of standard screen printed electrodes. These microfabricated electrodes make it possible to use small solution volumes and with systematic dilutions impedance spectra can be obtained from electrolytes having a large range of ionic conductivities [13].

Previous studies have used equivalent circuit models to analyze the impedance behavior of electrolytic solutions. Sanabria et al. examined an equivalent circuit model with three segments corresponding to the electrode/electrolyte interface, the electrolyte itself, and the impedance from the cabling of the instrument [14]. Their model consisted of a parallel resistor and capacitor in series with a constant phase element, resistor, and inductor. The resistor and capacitor were used to model the conductive electrolyte, the constant phase element was used for the polarization impedance of the electrodes, and the resistor and inductor combination represented the impedance from the cabling of the potentiostat. Lima et al. later refined this model to include an additional capacitive component in parallel with the constant phase element, corresponding to a double layer of ions at the electrode surface [15].

A number of previous studies have examined the impedance of PEDOT and have proposed circuit models to explain their behavior.[16–19] Bobacka et al. proposed a three element model including a solution resistance, diffusion impedance, and bulk capacitance. Montero-Rodríguez examined six different circuit models for PEDOT-coated electrodes and used a chi-squared fit to determine the best model. [15] Their best fit was obtained with a five-element model that was an extension of the Bobacka model with an additional double layer capacitor and charge transfer resistor. However there was limited experimental work done to determine how these complex models related to variations of the physical components of the system.[16,17,20–22]

In this work we performed impedance spectroscopy measurements using a variety of commercially available screen-printed electrodes on solutions of controlled solution conductivity. The impedance changes brought upon by changing instrumentation as well as the working electrode surface through PEDOT deposition gave us a large selection of impedance data for critical examinations of equivalent circuit models. The dependence of each element on the various components of the system (solution, electrode surface, and PEDOT polymer) was demonstrated through the shifts in the low, intermediate, and high frequency components of the impedance spectra. Our results made it possible to precisely elucidate and quantify these influences on the resulting impedance response. We were also able to identify and isolate the influence of instrument limitations, which were found to be particularly dominant at the highest frequencies and the lowest solution conductivities.

Experimental Section

Standard conductivity solutions were purchased from Hach (Loveland, CO) with conductivities of 1E-2, 1E-3, 1E-4, and 2.5E-5 S/cm

Accepted Manuscript
Version of record at: https://doi.org/10.1002/celc.202200231

SPE	WE	CE	RE
220AT	Gold (12.56 mm^2)	Gold (9 mm^2)	Ag
C223AT	Gold (2 mm^2)	Gold (17.5 mm^2)	Ag
C223BT	Gold (2 mm^2)	Gold (17.5 mm^2)	Ag
110	Carbon (12.56 mm^2)	Carbon (9 mm^2)	Ag
150	Carbon (12.56 mm^2)	Platinum (9 mm^2)	Ag
550	Platinum (12.56 mm^2)	Platinum (9 mm^2)	Ag

Table 1. Ceramic screen-printed electrode characteristics

respectively for sodium chloride (NaCl) and 1.113E-1, 1.2890E-2, 1.412E-3, 1.469E-4 S/cm for potassium chloride (KCl). The NaCl solutions were then each diluted in a 1:1 dilution with DI water three times to give 50%, 25%, and 12.5 % of the salt concentration/solution conductivity of the original solution. All measurements were done as at least duplets to check for reproducibility using droplets with a volume of 75 µL. The frequency response analysis measurements were done on a Metrohm Autolab PGSTAT128N from 1 Hz to 500 kHz with a 0 V applied potential vs reference and 10 mV oscillation amplitude. Further instrument impedance analysis was done with the PGSTAT128N as well as an Ametek Solartron Analytical and Gamry Reference 600 using an impedance range of 0.1 Hz to 1 MHz using the standard solutions NaCl solutions with the C223AT electrode.

Variations in electrode material and area were also tested with commercially available Metrohm / Dropsens electrodes having different materials (gold, platinum, and carbon) as the working electrode (WE) and counter electrode (CE) with a constant silver pseudoreference electrode (Table 1, Figure S1). Based on manufacturer specifications this is -0.131 V vs. Ag/AgCl. The geometry changes ranged from a WE:CE area ratio of 1.40 for the 220AT, 550, 150, and 110 to 0.114 for the C223AT and C223BT.

0.01 M EDOT with 0.02 M lithium perchlorate ($LiClO_4$) was electrochemically polymerized in an 88:12 by volume water:propylene carbonate (PPC) co-solvent mixture. Neat PPC was used to first dissolve the EDOT followed by subsequent addition of water and $LiClO_4$. Sonication for 15 minutes and vortexing for 30 seconds prior to deposition yielded a homogeneous solution. Potentiostatic deposition at 1.1 V vs. the silver pseudoreference electrode for an injected charge density of 0.755 C/cm^2 yielded consistent PEDOT films estimated at 1 µm of thickness [23,24]. Impedance measurements were done with the four standard solutions with no dilution.

Results

Impedance Changes from Solution Conductivity

Solution conductivities were determined from the impedance using the Bode plot of the spectra where the amplitude of the impedance is related to frequency. On a log scaling of both the x and y axes there was a region with minimal impedance change that corresponded to the resistance from the solution, hereafter called the frequency independent region. In a large enough frequency area there could be determined a point at low and high frequency that defined transitions to frequency dependent regions[1]. The frequency dependent regions were due to the onset of capacitive effects as will be discussed later.

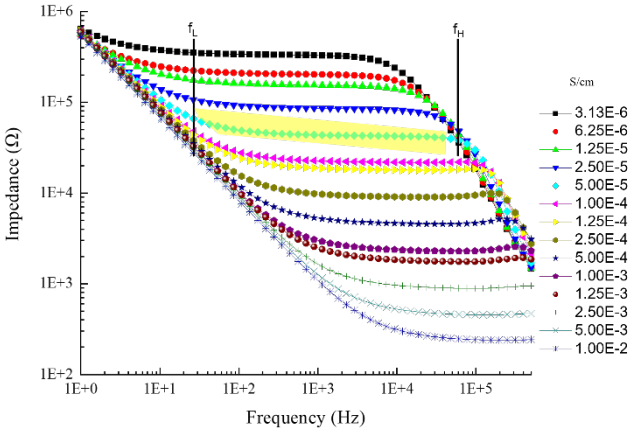

Figure 1 Bode plot with respect to conductivity. Highlighted region with markings for f_L and f_H of the frequency independent region (R) are given for the 5E-5 S/cm curve.

For each of the solutions tested, the impedance showed a relatively frequency independent resistive response over a range of frequencies. For the lower conductivity solutions (higher overall impedance) we saw both a low frequency transition (f_L) to frequency-dependent (capacitive) regime, and a high frequency transition (f_H) to another frequency-dependent regime (Figure 1). For the highest concentration solutions, the transition at high frequency (f_H) was not observed because it was presumably out of the range of our instrumentation (maximum frequency 500 kHz).

As solution conductivity increased the impedance systematically decreased as expected for the frequency independent region (Figure S2). We also found that the values of both f_L and f_H increased with increasing conductivity (Figure 1). The high frequency transition f_H did not increase as fast with solution conductivity compared to the f_L (Figure 3).

Using the average impedance of the solution conductivity region a calibration curve was constructed (Figure 2). A log input of conductivity provides a log output impedance which can then be transformed into an impedance of Ohms. The inverse provided

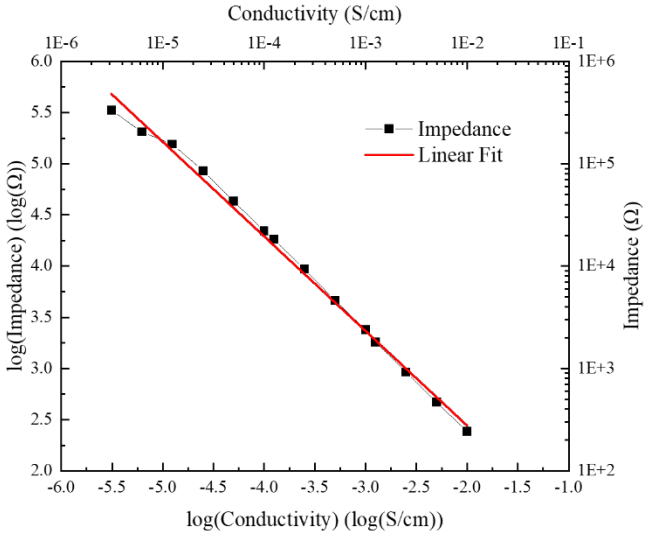

Figure 2. Impedance calibration curve to solution conductivity with linear regression

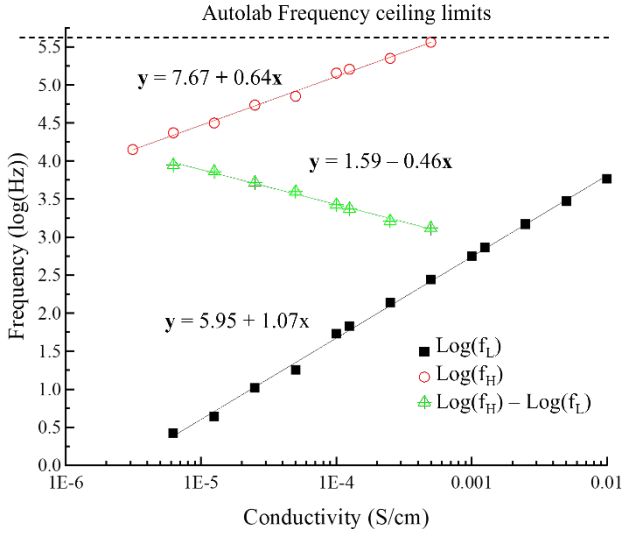

Figure 3. Change in the start and end frequency of solution conductivity region and the difference between

a calibration equation for determination of solution conductivity from the impedance of solution. The ability to determine solution conductivity from impedance spectra using simple screen-printed electrodes has been useful as our group has started looking into liquid mixtures composed of synthesized functional EDOT monomers available in small quantities. This approach is essentially similar to the calculation of a cell constant K_{cell} for interdigitated electrodes [25]. Our results give a value of K_{cell} = 1.97 cm^{-1}.

The Bode plots showed a frequency-dependent (capacitive-dominated) response at low frequencies, an essentially frequency independent response at intermediate frequencies, and another frequency-dependent (capacitive-dominated) response at higher frequencies. As discussed earlier, we defined the low frequency transition as f_L and the high frequency transition as f_H (Figure 1). The values of f_L and f_H were determined by analyzing the 2nd derivatives of the Bode plot with respect to frequency (Figure S3). Figure 3 illustrates the changes in log f_L and f_H as a function of solution conductivity. Both f_L and f_H increased with solution conductivity σ, however the scaling of the response was different. The low frequency transition increased as $\sim\sigma^a$ with a = 1.06, whereas the high frequency transition showed a = 0.64. Since f_H increased more slowly with σ than f_L, the difference between f_L and f_H (f_H - f_L) decreased with σ according to a= -0.46. Again, the data was limited by the high frequency maximum range (500 kHz) of the instrument (Table S1).

Electrode Variation

Figure 4 shows impedance for a range of different electrode compositions and surface areas. In all cases, we again saw frequency-dependent responses at high and low frequencies, and a range of resistive-dominated (frequency independent) behavior at intermediate frequencies. The overall changes in electrochemical impedance spectra based on increasing impedance from decreasing area of the working electrode correlated well with previous studies that found the same trend [24]. This caused a grouping due to large electrodes (220AT, 110, 150, 550) at low impedances compared to the high impedances for the small electrodes (223AT and 223BT), Figure 4. The working electrode material had a minimal effect on all the impedance spectra except for those of the highest conductivity solutions where impedances were already low. When the impedances were low, the spectra were more sensitive to differences in electrode material and surface coatings. Specifically, carbon working electrodes (110 and 150) suffered from increased impedance in the frequency independent region. 220ATs matched well with their groupings at middle to high frequencies, but in all conductivity solutions had unique low frequency impedance. Changes in the counter electrode material was found to have negligible effects compared to changing the working electrode. The overall shape of the Bode plots were the same with changes occurring on the impedance magnitude and the high and low frequency transitions.

Comparisons of the low and high frequency transitions and length of the frequency independent region showed the same response as noted from Figure 3 with f_H and f_L both increasing with conductivity, and their difference decreasing. As expected from the Bode plots the dependence of impedance on solution conductivity was generally similar for all electrodes except for the 110 and 150 (Figure S5). The slopes and intercepts of the linear fits (Table S2) were similar to those given in Figure 2 except for those of the 110 and 150. However, by eliminating the high solution conductivity inconsistencies all electrodes had a similar

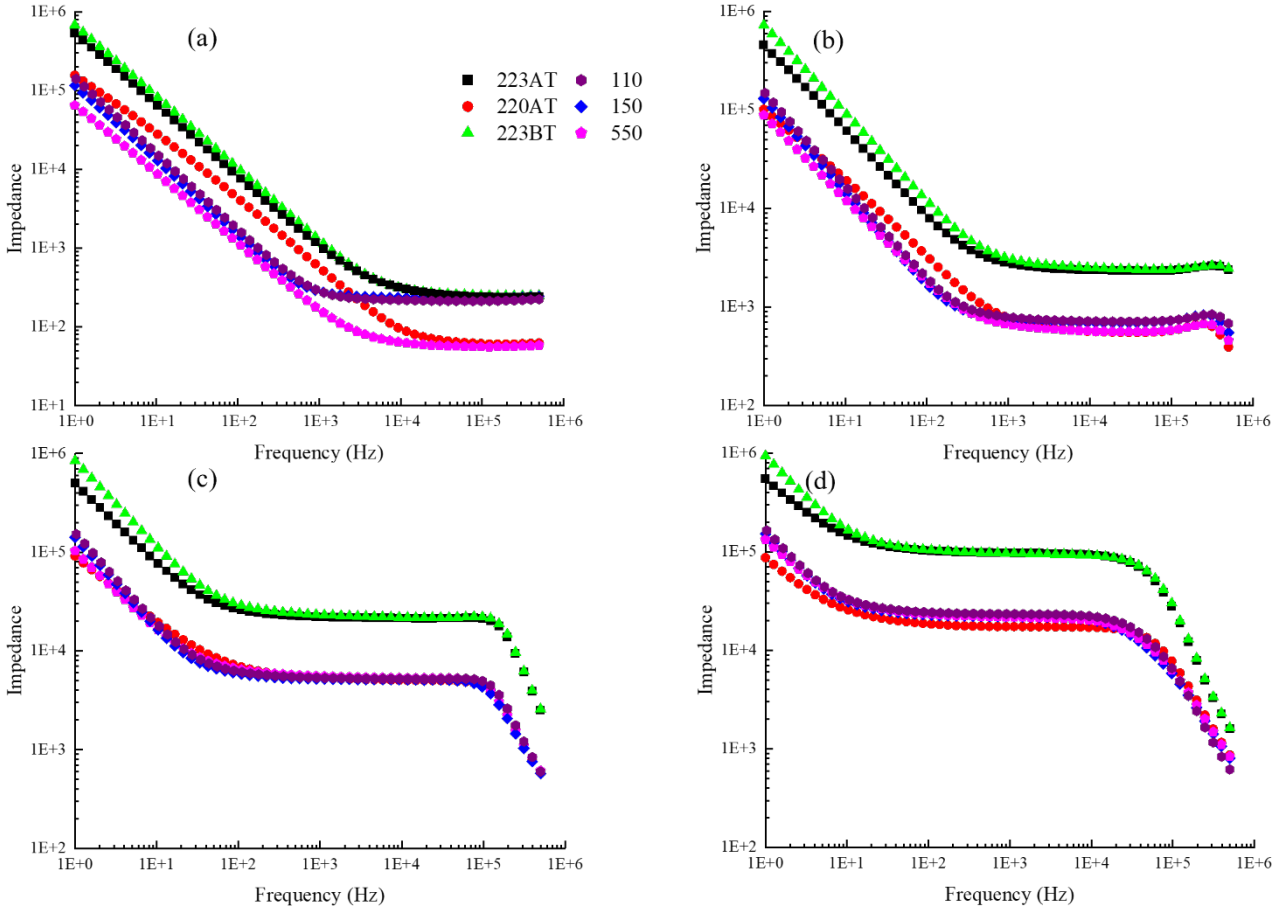

Figure 4. Variation in electrode size and composition in (a) 1.00E-2 S/cm, (b) 1.00E-3 S/cm, (c) 1.00E-4 S/cm, and (d) 2.50E-5 S/cm NaCl solutions

Accepted Manuscript
Version of record at: https://doi.org/10.1002/celc.202200231

slope with an average of -1.05 ± 0.028 (Table S2 and Table S3).

Examination of the f_L and f_H showed a dependence on both material and area of the working electrode (Figure S6). For the 110 and 150 SPEs removing the highest conductivity f_L was found to bring the slope in close agreement with the majority of the other measurements again showing that the carbon SPEs had changes in behavior in high conductivity solutions (Table S4). The slopes for f_H were also in close agreement between 0.68 and 0.78. As an outlier to the rest, the 220AT had the highest $f_{L,slope}$ at 1.24 and lowest $f_{H,slope}$ at 0.548. Looking at the difference in slopes showed that the small area electrodes frequency independent regions grew slowest with conductivity as solution conductivity increased while the 220AT frequency independent region grew fastest with solution conductivity.

Ion Composition

Changing to a larger ion size of potassium chloride from the sodium ion used showed no significant deviations from the expected general shape of the impedance curves or the labeled transitions of f_L and f_H (Figure 5). The potassium chloride impedance curves' frequency independent regions fit directly in line with the sodium chloride curves as a function of solution conductivity. This makes intuitive sense as solution conductivity depends directly on the ionic strength of the of the solution which was the main source of control in this study. Some low frequency deviations were observed and are discussed in more detail in the following section on equivalent circuit modeling.

Ion size can have effects on the solution conductivity where increasing ion size increases overall mobility and ionic conductivity.[26] Simple salts show linear increases of conductivity with respect to concentration, but extremely large, complex salts may have lower mobility, particularly in electrodes with small pore sizes. Reactive salts, ions, or other undesired electroactive impurities can cause changes in impedance spectra as the solution ion concentration changes. This may become important in cases where a solution is used for both impedimetric and electrochemical experimentation as is the case for electrochemical deposition of PEDOT which incorporates anions when oxidized.[27]

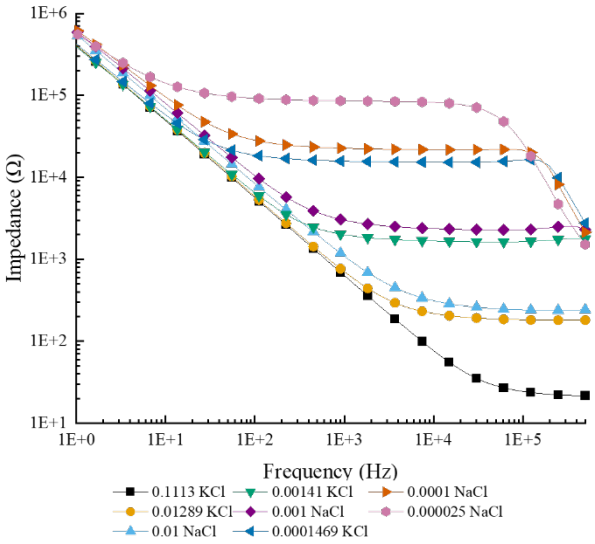

Figure 5 Solution conductivity ion variation. Units are in S/cm with the ion details besides.

Instrument Variations

Studies from the literature do not typically focus on high frequency data (1E4 Hz and higher) from impedance spectra due to potential contributions from instrument artifacts [28,29]. Here we used three different potentiostats (Autolab Potentiostat 128N, Ametek Solartron Analytical, and Gamry Reference 600) and verified the strong dependence of high frequency impedance response to the specific instrumentation used (Figure 6). The low to middle frequency regions remained generally unchanged whereas the high frequency transition f_H and the following capacitive region both changed substantially. At the highest frequencies the responses for a given instrument all collapsed down to values that evidently correspond to the intrinsic impedance of a particular device. As we discuss later, the instrument component of the impedance that becomes dominant at high frequencies is described well by a constant phase element. While a given potentiostat may be able to reach high magnitudes of frequency, determination of the representative element gives a better idea as to the functional frequency ceiling for a given solution conductivity.

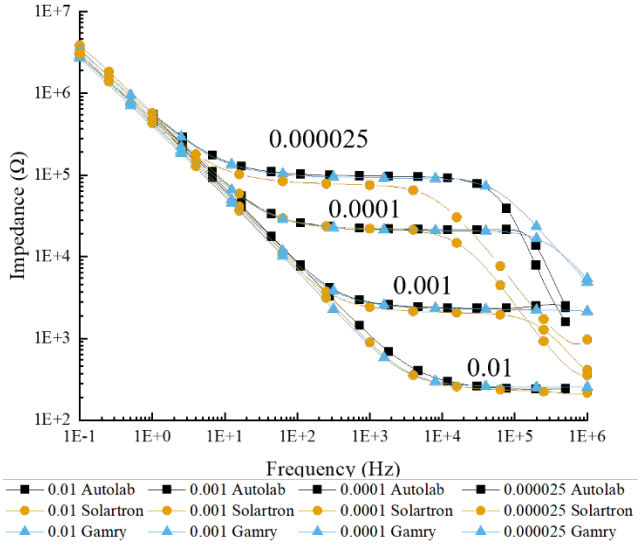

Figure 6 Solution conductivity instrument variation. Units are in S/cm with the details instrument besides.

PEDOT Deposition Effects

PEDOT deposition onto the C223AT screen printed electrodes had a drastic effect on lowering the impedance mainly in the low frequency region as shown in Figure 7. Because of this the low frequency transition f_L decreased by about two orders of magnitude, while the high frequency transition remained essentially the same for samples with and without PEDOT. This broadened the frequency range of the solution conductivity region and the low frequency capacitive region now converged at lower overall frequencies.

In the mid-to-high frequency regions the change in impedance was minimal due to it being dominated by the solution conductivity and instrument dependent impedance effects and therefore was mostly unchanged with PEDOT polymerization. Minimal impedance changes were likely due to the increase in effective surface area of the working electrode due to the rough, bumpy structure of PEDOT [18]. The deposited PEDOT widened the frequency independent region by nearly two orders of magnitude compared to that of the bare SPE at all solution conductivities (Table S1).

Comparing the magnitude of the change in impedance between the bare screen-printed electrodes and PEDOT deposited electrodes emphasizes the changes that solution conductivity brings to the decrease in impedance of the system

Accepted Manuscript
Version of record at: https://doi.org/10.1002/celc.202200231

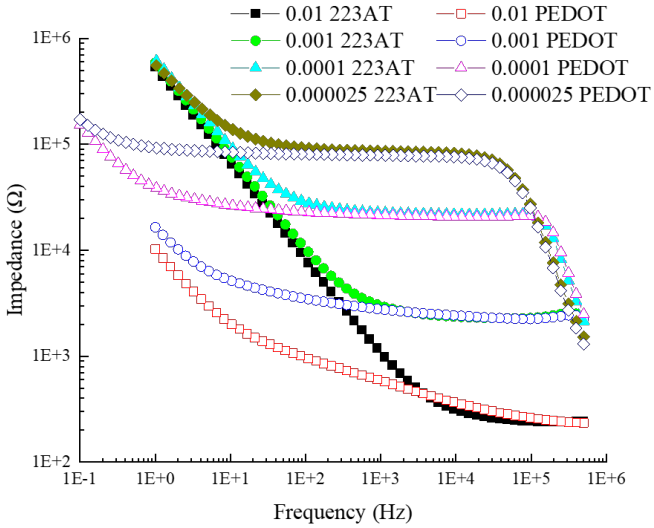

Figure 7 PEDOT impedance behavior on 223AT in 1E-2 S/cm, 1E-3 S/cm, 1E-4 S/cm, and 2.5E-5 S/cm NaCl solutions

(Figure 8). Differences in scaling provides context for what changes in impedance are significant. Figure 8 (left and right) showed an impedance decrease at low frequency as is clear from the Figure 7 when comparing the Bode plots, but at 1 kHz (the frequency often examined closely for biomedical interfacing) the degree in drop varies significantly. For the low conductivity solutions (Figure 8 (left)) there was a negligible difference while in high conductivity solutions there was a 0.3 order of magnitude decrease. Numerical differences (Figure 8 (right)) showed the opposite effect where low conductivity solutions showed the largest change of roughly 10 kΩ and high conductivity solutions showed an impedance change of roughly 100 Ω. Examination of just a single frequency under differing solution conditions and scaling can clearly lead to dissimilar conclusions on the impedance changes. For all solution conductivities the difference in impedance of log(Ω) with frequency leads to convergence at high frequencies while the difference in impedance of Ω with frequency leads to convergence at low frequencies.

Equivalent Circuit Modeling

Previous work on modeling of simple gold electrodes in the context of conducting polymers found that a two-element equivalent circuit model using a resistor and capacitor in series was sufficient for a good fit [24]. In this work we found that for the lowest frequency regions (10^4 Hz and below) this model was reasonably accurate for all solution conductivities when compared to the Bode plots, but varied significantly when taking into examining the Nyquist plots . Changing the capacitor to a constant phase element significantly improved the overall fit. Constant phase elements have a magnitude T and phase factor P that varies from 0 and 1 depending on the degree of resistive (P = 0) to capacitive (P = 1) behavior.

In our system the constant phase element 1 (CPE1) was found to represent the interfacial impedance between that of the solid electrode (metal) surface and the liquid electrolyte. This element was affected by both the interfacial material as shown by depositing PEDOT and by changing the electrode size as seen by comparing the 2 mm^2 and 12.56 mm^2 electrodes. CPE1 was responsible for the low frequency behavior of the impedance curves and the transitions to the flat, frequency independent region at f_L.

The resistor element impedance (R, frequency independent region) correlates to the solution conductivity and was therefore dependent on the ionic strength of the solution (i_S), the surface area of the electrodes (A), and the distance between the electrodes (d) as shown in Equation 1. This was the most obvious of the changes on the impedance spectra as ionic strength (NaCl concentration) was varied while both area and distance were held constant when using exclusively the C223AT electrode. R is the dominant element for the intermediate frequency region between CPE1 and CPE2.

$$R = {}^{d}/_{A\, i_S} \quad (1)$$

The constant phase element 2 (CPE2) represents the impedance due to the specific potentiostat used (instrumental limitations). As R decreases, the point where CPE2 and R meet, f_H, shifts to higher frequencies and goes out of the working impedance frequency region for the given potentiostat. For this reason, CPE2 was not used when modeling high conductivity (≥5,000 µS/cm) solutions.

An additional Warburg element relating to ionic diffusion in PEDOT films has been used in previous studies[18]. We found that this particular circuit element was not necessary to get good fits to our experimental results.

The points where the individual elements met, labeled as f_L and f_H, shifted as a function of the changes in the elements used. Variables of R, T_x, and P_x, where x = 1 for CPE1 and x =2 for

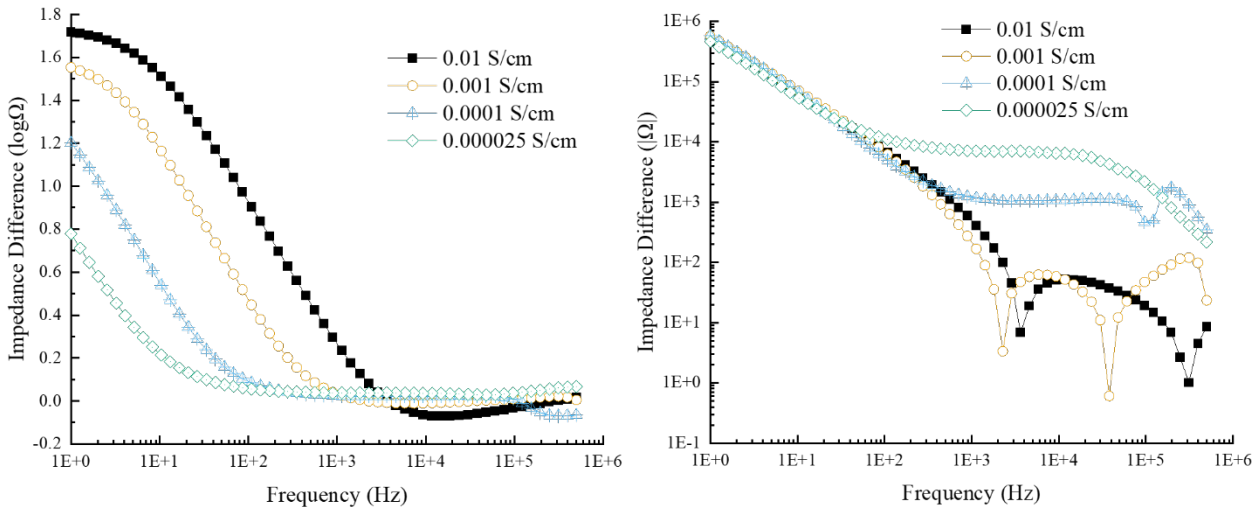

Figure 8 Difference in (left) order of magnitude and (right) absolute value of bare and PEDOT functionalized 223AT SPE

CPE2 were used to define the elements outlined in Equations 2 and 3 with frequency (ω) as the independent variable (notation used as seen in Zview).

$$Z_R = R \tag{2}$$

$$Z_{CPE_x} = \frac{1}{T_x(i\omega)^{P_x}} \tag{3}$$

At the low frequency transition the impedance contributions from CPE2 are negligible which means that is the point where R and CPE1 are equal. Combining equations 2 and 3 (with x=1) and solving for ω gives equation 4 for f_L:

$$f_L = \frac{\omega_L}{2\pi} = \frac{(RT_1)^{-1/P_1}}{2\pi} \tag{4}$$

Here f_L is the low frequency transition in Hz, ω_L is its value in radians/sec, R is the solution resistance, T_1 is the amplitude of CPE1 describing the interfacial resistance, and P_1 is the phase of CPE1. Likewise, we can solve for f_H by combining equation 2 with 3 (with x=2), giving:

$$f_H = \frac{\omega_H}{2\pi} = \frac{(RT_2)^{-1/P_2}}{2\pi} \tag{5}$$

Similarly, f_H is the high frequency transition in Hz, ω_H is its value in radians/sec, R is again the solution resistance. T_2 is now the amplitude of CPE2 describing the instrument impedance, and P_2 is the phase of CPE2.

The impedance spectra were fitted using Zview 3.5g to determine the related variables described previously. As expected from the plots there was a decrease in solution resistance R with both increasing solution conductivity and working electrode size (Figure S7a and Figure S8a). For CPE1-P the phase increased with solution conductivity for all electrode types. From the 223AT curve the maximum reached at high conductivity corresponded to a more capacitive interface with more mixed behavior in low conductivity solution giving a minimum (Figure S7c). The phase behavior in this case corresponded to a leaky double layer ionic capacitor [30,31]. Increasing solution conductivity increased the phase angle as the availability of more ions formed a better double layer capacitor. This CPE1-T showed a fairly constant impedance for the small working electrode 223AT and BT but did start to show variations significantly for the 220AT as solution conductivity changed (Figure S8b). The combination of decreasing CPE1-T and overall lower CPE1-P caused the 220AT to differ from the rest of the electrodes at low frequencies. Larger KCl ions on the 223AT showed similar behavior for R and CPE1-P in line with NaCl solutions. The CPE1-T was increased which lowered the overall impedance at low frequencies.

As stated previously, high impedance data is generally not used for data analysis due the presence of instrument artifacts and effects. For CPE2-T and CPE2-P a variety of behavior was seen, but for a variety of electrodes with few data points no clear trend was determined (Figure S8d and S8E). The 223AT showed a minimum in CPE2-T and at the same solution conductivity of 1E-4 S/cm there was also a maximum in CPE2-P (Figure S7d and S7e). In all cases the phase behavior P was greater than one which is indicative of an instrumental artifact since it is out of the limits of P as defined earlier. As a result we sometimes saw evidence for atypical behavior in the Nyquist plot, with data points appearing in the top left quadrant.

Functionalization of the 223AT surface with PEDOT was found to work reasonably well with the given circuit model, but upon closer examination showed some small deviations at low frequencies. All the elements previously described were still there and the addition of PEDOT with its ability to store charge added a capacitor to the circuit. Figure 9(c) shows a low conductivity circuit with the capacitive PEDOT element added in series. High conductivity systems followed the same trend as Figure 9(a) and omitted CPE2 which appeared at too high of a frequency for the spectra.

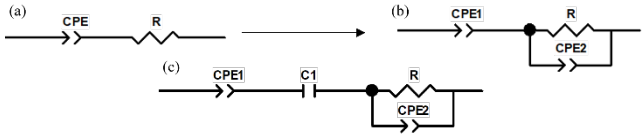

Figure 9 Equivalent circuit models for screen printed electrode systems at (a) high conductivity (≥ 5E-3 S/cm), (b) low conductivity (< 5E-3 S/cm) circuit model, and (c) low conductivities (< 5E-3 S/cm) with PEDOT

Comparisons of elements R and CPE1 from 9(b) and 9(c) showed minor decreases in the solution resistance and major changes in both CPE1-T and CPE1-P. PEDOT's rough and bumpy morphology is known to increase the electroactive surface area of the deposited electrode and minorly decreased the measured solution resistance [18]. The increase in electroactive surface area from PEDOT in this case was also minimal which resulted in a decrease in solution resistance at all solution conductivities. The magnitude of ohmic change was largest in low conductivity solutions and smallest in high conductivity solutions while the percentage change is largest at high conductivities and lowest for low conductivity solutions (Table 2). CPE1-P goes from 0.7-0.9 for a 223AT down to 0.4 for a PEDOT deposited 223AT. The impedance behavior of the interface for represented by CPE1 goes from being a leaky capacitor to a system with electrode to solution charge transfer enabled by the ion mobility between PEDOT and the ionic solution. An increase in solution conductivity decreases the phase angle for PEDOT interfaces as the availability of ions allows for faster charge transfer becoming more like a resistive interface. The doped nature of PEDOT provides a pathway for the ionic to electronic charge transfer that is enabled by excess ions. CPE1-T increases significantly which corresponds to a drop in impedance with both the addition of PEDOT and solution conductivity. PEDOT's effective volume allowed for the formation of a larger ion double layer which again increases with the ion concentration and accessibility. By adding PEDOT we have in essence taken our base electrode that was effectively a leaky capacitor and provided a streamlined pathway for the leakage current that provides a low impedance for CPE1.

PEDOT added a capacitive element to the circuit that changed minimally and inconsistently with changes in solution conductivity. This corresponds well to literature for PEDOT acting as an electronic capacitor in addition to the ionic capacitance effects shown in CPE1 [16,18]. As expected, the changes in CPE2 with PEDOT deposition were inconsistent since PEDOT does not change the functionality of the potentiostat used.

The equivalent circuit model used here provides a simple, detailed model with each element being clearly adjusted to show its dependence on a real-world experimental piece. One major difference with this model compared to previously used models is the use of a constant phase element instead of a parallel resistor and capacitor for charge transfer resistance and double layer

Rs (Ω)	Rs PEDOT (Ω)	Impedance decrease (Ω)	%Impedance decrease (Ω)
78360	72500	5860	7.483
20900	19120	1780	8.524
2321	1969	352.0	15.17
246.6	133.7	112.9	45.78

Table 2. Ohmic drop of solution resistance (Rs) impedance with PEDOT

capacitance respectively [18,20]. As opposed to two separate processes this implies that the charge transfer and double layer capacitance are not completely independent, use the same ions, and act as part of the same process. Previous models traditionally rely on theory combined with complex models that include many elements and do not necessarily look at all the fits between Nyquist, Bode magnitude, and Bode phase plots as well as experimentally manipulating individual pieces of the circuit [20]. Increasing the number of elements will make a better fit but will reduces the model's overall real-world accuracy as it becomes more difficult to isolate and identify specific elements for precise electrical interactions to their real-world components. This paper endeavors to provide in depth analysis of an equivalent circuit model and the changes brought upon it through altering various electrochemical experimental conditions. Fits done to the Bode and Nyquist plots from the data set in this work fit very close with both gold SPE and PEDOT coated gold SPE (Figure S9 and S10). Equivalent circuit model fit parameters are given in Table S5.

Discussion

An important question of concern is the appropriate range of solution conductivities that should be used in a given electrochemical experiment. If a specific range of frequencies are important then it is important to establish that the choice of electrode geometry and solution conductivity are such that the system responds appropriate over these time scales. In the case of bioelectronic interfacing the important frequencies of interest are typically 1 kHz and below. As shown in the data, there are two dependencies of impedance on solution conductivity. The first is the overall impedance of the system based on the ionic content and the second is the location of the frequency independent region. For commercially available phosphate buffered saline, a common medium used for biological comparisons, the solution conductivity is 15-20 mS/cm. This conductivity puts the 1 kHz frequency used for bioelectronics in the constant phase element of the impedance curve. Comparatively the conductivity in tissue ranges from 15.38 mS/cm for cerebrospinal fluid down to 62.5 µS/cm for hard bone [32]. In this case the 1 kHz frequency rests in the transition section from a more capacitive to resistive region.

By adjusting the solution of the impedance measurement, it is possible to misinterpret data as showing greater changes in impedance. Through use of a high conductivity solutions, it is possible to say there was a multiple order of magnitude drop in impedance when the change was only a few ohms. Conversely using a low conductivity solution will show a tens of thousands ohmic drop in impedance, but when scaled to what the electrode impedance is naturally, this drop is insignificant. The solutions used for measuring the impedance of conductive polymer solutions vary from solutions of 0.1 NaCl [24] to 1x PBS [33] to 0.5 M H_2SO_4 [34] as well as not being specified at all [11]. Table S6 lists some recent publications with some impedance characteristics listed using different electrode materials and electrode surface areas. As shown in Figure 4, both material and size play a part in impedance measurements and are not generally tailored for easy literature comparison. An added complication of conductive polymers grown electrochemically is the use of the deposition solution for impedance measurement. As deposition continues the solution itself will lose solute from deposition that will affect conductivity and therefore impedance measurements. Impedance measurements should ideally be done in inert salt solutions or some other well controlled system as use of the monomer deposition solution will include reactive chemicals.

Table S7 lists a variety of impedance characteristics taken from papers in the literature that focus on electrochemical impedance for use with SPE's. In many cases these papers reference each other or are referenced for use in looking at similar systems and procedures in fields such as glucose oxidase sensing. Impedance characterization utilize a variety of solutions such as DI water [35,36], 0.1 M KCl with $[Fe(CN)_6]^{4-/3-}$ redox probes at various concentrations [37–40], and various PBS concentrations [41–43]. The reported impedance spectra are then used for sensing measurements without considering the spectra changes from solution conductivity.

Observations from this work and literature have clearly shown that measuring the impedance magnitude at a single given frequency does not make it possible to understand the complicated dynamics of interfacial electronic and ionic charge transport in these systems, particularly when the concentration and composition of the electrolytes are changing. The impedance magnitude at a given frequency is simple to measure but can be easily varied by effects from the measuring solution. The frequency independent impedance floor created by the solution resistance causes intrinsic limitations of how much the impedance can drop from coating with conductive polymer.

Understanding the circuit model and using the transition points provides improved metrics such as f_H and f_L that are dependent on more than solution conductivity. Calculating the frequency drop in f_L provides a useful idea of how much PEDOT coatings change the overall impedance of the system. Large decreases in f_L allow for a wider regions of the impedance spectra to be dominated by the inherent electrolytic solution conductivity.

The best way to make an ideal impedance spectrum with the lowest impedances over the widest range of frequencies requires adjusting multiple equivalent circuit elements. Increasing T and lowering P for CPE1 respectively lowers the impedance in the frequency range around f_L and decreases the frequency dependent nature of the impedance for this element. CPE1, like a capacitor, has an inverse relationship between frequency and impedance. By making this element more frequency independent the impedance increases at low frequency are drastically lowered. Increasing C, the capacitance due to PEDOT, will further decrease the impedance at low frequencies as the C element is the low frequency, high impedance boundary for the system in a Bode plot.

The f_L and f_H transitions for the proposed model are dependent on T and P for a constant phase element or C for a capacitor and the solution conductivity R. Adjusting R by using dilutions of salt solutions adjusts f_L and f_H as shown in Figure 3 as both CPE1 and CPE2 are kept constant. Increasing of T, C, and R as well as decreasing P leads to lower f_L PEDOT coatings having a high capacitance (C) element.

Conclusions

We have found that the impedance of salt solutions shows a relatively flat, resistive behavior corresponding to the solution resistance R over a range of intermediate frequencies between f_L and f_H. The lower characteristic frequency f_L corresponds to the point where the interfacial impedance Z_{CPE1} is equal to R, whereas the higher frequency f_H corresponds to the point where the instrument impedance Z_{CPE2} is equal to R. For a given solution resistance R, lowering the interfacial impedance Z_{CPE1} will result in a decrease of f_L, as shown by equation 4. Similarly, increasing the impedance of the instrument Z_{CPE2} will lead to a decrease of f_H by equation 5.

Here, electrochemical impedance spectroscopy was used to analyze the relation between impedance, frequency, and solution conductivity for coatings of conjugated polymers on metallic electrodes in the presence of salt solutions. Our results have made it possible to identify the impact of the electrolyte, interfacial coating, and instrument response on the experimental spectra. These insights should help to guide the optimization of these coatings for biosensing applications.

Acknowledgements

This work was supported in part by the National Science Foundation (DMR-180848), the AFOSR (MSIT Program for Next Generation Nanosystems), and the University of Delaware. Thanks to Shrirang and Yuhang for their help in editing.

Conflict of Interest

There are no conflicts to declare.

Keywords: Electrochemistry • Interfaces • Impedance Spectroscopy • Conducting Polymers • poly(3,4-ethylenedioxythiophene) (PEDOT)

[1] J. Hubálek, *Sensors* **2015**, *15*, 12080–12091.
[2] K. B. Chin, M. G. Buehler, S. Seshadri, D. Keymeulen, R. C. Anderson, S. Dutz, S. R. Narayanan, *Rev. Sci. Instrum.* **2007**, *78*, 016104.
[3] S. Arndt, J. Seebach, K. Psathaki, H.-J. Galla, J. Wegener, *Biosens. and Bioelectron.* **2004**, *19*, 583–594.
[4] H. P. Schwan, in *Advances in Biological and Medical Physics* (Eds.: J.H. Lawrence, C.A. Tobias), Elsevier, **1957**, pp. 147–209.
[5] D. C. Martin, *MRC* **2015**, *5*, 131–153.
[6] D. Kim, I. Zozoulenko, *J. Phys. Chem. B* **2019**, *123*, 5160–5167.
[7] H. Yano, K. Kudo, K. Marumo, H. Okuzaki, *Sci. Adv.* **2019**, *5*, eaav9492.
[8] E. Musk, *bioRxiv* **2019**, 703801.
[9] K. M. Reza, A. Gurung, B. Bahrami, S. Mabrouk, H. Elbohy, R. Pathak, K. Chen, A. H. Chowdhury, M. T. Rahman, S. Letourneau, H.-C. Yang, G. Saianand, J. W. Elam, S. B. Darling, Q. Qiao, *J. Energy Chem.* **2020**, *44*, 41–50.
[10] F. Torricelli, D. Z. Adrahtas, Z. Bao, M. Berggren, F. Biscarini, A. Bonfiglio, C. A. Bortolotti, C. D. Frisbie, E. Macchia, G. G. Malliaras, I. McCulloch, M. Moser, T.-Q. Nguyen, R. M. Owens, A. Salleo, A. Spanu, L. Torsi, *Nat. Rev. Methods Primers* **2021**, *1*, 1–24.
[11] B. Wu, B. Cao, I. M. Taylor, K. Woeppel, X. T. Cui, *Front. Chem.* **2019**, *7*, 178.
[12] M. Antensteiner, M. R. Abidian, in *39th Annu. Int. Conf. IEEE EMBC*, **2017**, pp. 1881–1884.
[13] C. S. Widodo, H. Sela, D. R. Santosa, in *AIP Conf. Proc.*, East Java, Indonesia, **2018**, p. 050003.
[14] H. Sanabria, J. H. Miller, *Phys. Rev. E* **2006**, *74*, 051505.
[15] L. F. Lima, A. L. Vieira, H. Mukai, C. M. G. Andrade, P. R. G. Fernandes, *J. Mol. Liq.* **2017**, *241*, 530–539.
[16] J. Bobacka, A. Lewenstam, A. Ivaska, *J. Electroanal. Chem.* **2000**, *489*, 17–27.
[17] P. Danielsson, J. Bobacka, A. Ivaska, *J. Solid State Electrochem.* **2004**, *8*, 809–817.
[18] M. Bianchi, S. Carli, M. D. Lauro, M. Prato, M. Murgia, L. Fadiga, F. Biscarini, *J. Mater. Chem. C* **2020**, *8*, 11252–11262.
[19] S. Carli, M. Bianchi, E. Zucchini, M. Di Lauro, M. Prato, M. Murgia, L. Fadiga, F. Biscarini, *Adv. Healthcare Mater.* **2019**, *8*, 1900765.
[20] J. J. Montero-Rodrıguez, D. Schroeder, W. Krautschneider, R. Starbird, in *6th IEEE Ger. Stud. Conf.*, **2015**, p. 5.
[21] J. R. Macdonald, *Electrochim. Acta* **1992**, *37*, 1007–1014.
[22] X.-Z. Yuan, C. Song, H. Wang, J. Zhang, Eds. , in *Electrochemical Impedance Spectroscopy in PEM Fuel Cells: Fundamentals and Applications*, Springer, London, **2010**, pp. 139–192.
[23] S. Nagane, P. Sitarik, Y. Wu, Q. Baugh, S. Chhatre, J. Lee, D. C. Martin, *MRS Adv.* **2020**, 1–14.
[24] D. A. Koutsouras, P. Gkoupidenis, C. Stolz, V. Subramanian, G. G. Malliaras, D. C. Martin, *ChemElectroChem* **2017**, *4*, 2321–2327.
[25] R. de la Rica, C. Fernández-Sánchez, A. Baldi, *Electrochem. Commun.* **2006**, *8*, 1239–1244.
[26] P. Kumar, S. Yashonath, *J. Mol. Liq.* **2019**, *277*, 506–515.
[27] I. Zozoulenko, A. Singh, S. K. Singh, V. Gueskine, X. Crispin, M. Berggren, *ACS Appl. Polym. Mater.* **2019**, *1*, 83–94.
[28] A. Sadkowski, J.-P. Diard, *Electrochim. Acta* **2010**, *55*, 1907–1911.
[29] F. Mansfeld, S. Lin, Y. C. Chen, H. Shih, *J. Electrochem. Soc.* **1988**, *135*, 906.
[30] C.-T. Chu, P. D. Fuqua, J. D. Barrie, *Appl. Opt.* **2006**, *45*, 1583–1593.
[31] "Basics of EIS: Electrochemical Research-Impedance," can be found under https://www.gamry.com/application-notes/EIS/basics-of-electrochemical-impedance-spectroscopy/, **2006**.
[32] C. Ramon, P. Schimpf, J. Haueisen, *Biomed. Eng. OnLine* **2006**, *5*, 10.
[33] S. Venkatraman, J. Hendricks, Z. A. King, A. J. Sereno, S. Richardson-Burns, D. Martin, J. M. Carmena, *IEEE Trans. Neural Syst. Rehabil. Eng.* **2011**, *19*, 307–316.
[34] V. Saunier, E. Flahaut, M.-C. Blatché, C. Bergaud, A. Maziz, *Biosens. and Bioelectron.* **2020**, *165*, 112413.
[35] J.-H. Park, C.-S. Kim, B.-C. Choi, K.-Y. Ham, *Biosens. and Bioelectron.* **2003**, *19*, 321–324.
[36] A. Tura, S. Sbrignadello, S. Barison, S. Conti, G. Pacini, *Biophys. Chem.* **2007**, *129*, 235–241.
[37] H.-P. Peng, Y. Hu, P. Liu, Y.-N. Deng, P. Wang, W. Chen, A.-L. Liu, Y.-Z. Chen, X.-H. Lin, *Sens. Actuators, B* **2015**, *207*, 269–276.
[38] P. Geng, X. Zhang, W. Meng, Q. Wang, W. Zhang, L. Jin, Z. Feng, Z. Wu, *Electrochimica Acta* **2008**, *53*, 4663–4668.
[39] M. Gamella, S. Campuzano, C. Parrado, A. J. Reviejo, J. M. Pingarrón, *Talanta* **2009**, *78*, 1303–1309.
[40] A.-E. Radi, J. L. Acero Sánchez, E. Baldrich, C. K. O'Sullivan, *Anal. Chem.* **2005**, *77*, 6320–6323.
[41] T. Leigh Adamson, F. Ang Eusebio, C. B. Cook, J. T. LaBelle, *Analyst* **2012**, *137*, 4179–4187.
[42] M. Varshney, Y. Li, *Biosens. and Bioelectron.* **2007**, *22*, 2408–2414.
[43] S. S. Low, H.-S. Loh, J. S. Boey, P. S. Khiew, W. S. Chiu, M. T. T. Tan, *Biosens. and Bioelectron.* **2017**, *94*, 365–373.

Accepted Manuscript
Version of record at: https://doi.org/10.1002/celc.202200231

RESEARCH ARTICLE

Entry for the Table of Contents

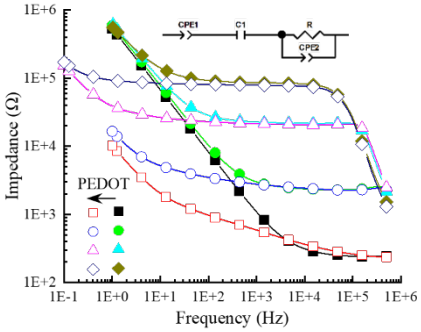

This work provides a detailed analysis and modeling of the impedance spectra for conducting polymers with a focus on how the equivalent circuit model changes with deposition of poly(3,4-ethylenedioxythiophene) (PEDOT) and changing solution conductivity.

Keywords: Electrochemistry, Polymerization, Conducting Materials, Interfaces, Conducting Polymers, Equivalent Circuit Modeling, Impedance Spectroscopy

Institute and/or researcher Twitter usernames: miltydcm (David C. Martin)